Effects of Thermal Annealing and Selective Chemical Etching on Structural and Optical Properties of GaAsBi Epilayer with Droplet Systems

Tulin Erucar, Kamuran Kara, Omer Donmez, Ayse Erol, Alexandre Arnoult, Chantal Fontaine

Effects of Thermal Annealing and Selective Chemical Etching on Structural and Optical Properties of GaAsBi Epilayer with Droplet Systems

Tulin Erucar[1], Kamuran Kara[1], Omer Donmez[1], Ayse Erol[1] , Alexandre Arnoult[2], and Chantal Fontaine[2]

[1]Department of Physics, Faculty of Science, Istanbul University, Vezneciler, 34134, Istanbul, Turkey
[2]LAAS-CNRS, Université de Toulouse, 7 Avenue du Colonel Roche, 31400, Toulouse, France

A GaAs1−xBix layer was grown by molecular beam epitaxy (MBE) with a low Bi content (2.3%) on GaAs maintaining the substrate at a non-rotating state and was then annealed at 750 C, 800 C and 850 C. Each sample that was covered with droplets was investigated by using the Atomic Force Microscopy (AFM), Electrostatic Force Microscopy (EFM) and Photoluminescence (PL) techniques. The surface properties of the GaAs1−xBix layer were investigated by AFM and observed to have a droplet system, which was composed of a donut and a tail. The optical quality of the samples was enhanced after thermal annealing up to 800 C, and the maximum PL intensity was obtained at 750 C. AFM images revealed that the shape of the droplet and tail changed with increasing annealing temperature. EFM images revealed a phase separation on the surface droplet system. To explore the nature of the droplets, previously claimed to be made of Ga and/or Bi, and their effect on PL spectrum, a chemical etch procedure was carried out by using diluted solutions of H2SO4 and/or HCl. We showed that droplets may be efficiently removed from the surface, and PL intensity could be improved by using a proper sequence of chemical etching procedures. Furthermore, the presence of two different phases for the droplet-system observed by EFM was also confirmed by the selective etching procedure.

Keywords: GaAsBi, Dilute Bismide, Droplet, Thermal Annealing, Chemical Etching.

1. INTRODUCTION

Incorporation of a few percent of Bi into GaAs efficiently shifts its bandgap energy down into the infrared range, which makes these alloys promising for optoelectronic devices for IR and MIR applications.1 2 Compositiondependent bandgap reduction was measured to be as high as 60–90 meV/Bi%.3 4 The attractiveness of GaAsBi alloys is also supported by their significant composition dependence on the Bi content of spin-orbit splitting energy3 and almost no temperature dependence of their bandgap.

These advantages have led to a significant research effort on these alloys. Much attention has been paid to their epitaxial growth, found to be more stringent than the growth of classical III–V semiconductor alloys, in particular by molecular beam epitaxy (MBE). Growth of good quality GaAsBi epilayers strongly depends on growth parameters such as Bi flux, V/Ga flux ratio and growth temperature. MBE-growth temperature has to be lower than 400 C to incorporate this large-sized element in GaAs lattice. At higher growth temperatures, Bi is no longer incorporated but can be used as a surfactant for GaAs and related alloys like GaNAs.5 Furthermore, the V/Ga flux ratio must be close to stoichiometry to have high structural quality in GaAsBi layers. When this ratio is too high, incorporation of Bi becomes inefficient.6 When this ratio is lower than unity, Ga droplets are formed. Pure Bi, Ga or Ga–Bi droplets on the surface of GaAsBi layers have been reported in Refs. [5, 7, 8] and Bi droplet formation has been proposed to be originated from the use of high Bi flux for its complete incorporation. There has been intense research on the growth kinetics of these materials and the growth-condition dependence of droplet formation on GaAsBi growing surfaces.9 10 An

understanding of the formation and effects of droplets on GaAsBi properties is mandatory to make these alloys suitable for their potential application areas.

Apart from their growth-condition-dependent properties, GaAsBi properties may suffer from the presence of Biclusters or alloy disorder due to their low-temperature growth. Post-growth thermal annealing has been shown to improve the optical and structural quality of MBE-growth GaAsBi alloys with 2.2% Bi up to 700 C,10–12 and likewise, for all highly mismatched alloys (HMAs).[5] There has been still a dilemma about the effects of thermal annealing on the bandgap of GaAsBi. By some groups, blueshift was reported,13 but there are also a few papers in which redshift was observed.14 15 Besides, in case of observation of a rather broad PL peak from GaAsBi, no shift of the bandgap of GaAs has been observed following thermal annealing.[9]

This paper investigated the effects of thermal annealing and selective etching on the optical and structural properties of a GaAsBi layer with a low Bi concentration (2.3%) and droplets at its surfaces by using AFM, EFM and PL measurements. The GaAsBi layer that was used in this study came from the edge of a wafer, whose droplet-free center has already been studied.11 We observed that thermal annealing profoundly affects PL intensity and droplet structure. The nature of the droplets was determined to be composed of both Ga and Bi. We showed that droplets may be efficiently removed from the surface by using two sequential chemical etching processes with H2SO4 and HCl. Following these chemical processes, PL emission intensity was observed to be increased.

2. EXPERIMENTAL DETAILS

The GaAsBi layer was grown on a piece of (001) GaAs by molecular beam epitaxy in a 2300 RIBER system. The (001) GaAs substrate piece was soldered with indium radially on a 3 inch-diameter silicon wafer. Firstly, a GaAs buffer layer was grown at 580 C, 1 ml/sec and under an As4 flux corresponding to two times the As4 flux needed for stoichiometric GaAs growth. The substrate holder was rotating during buffer growth. Then the growth temperature was lowered. The thermocouple temperature was fixed to get a real temperature of about 380 C. The substrate holder was kept immobile during GaAsBi growth. GaAsBi was grown at the speed of 0.25 monolayer/second and with minimal As4/Ga flux ratio to get GaAs stoichiometry. X-ray diffraction that was carried out with a Bruker D8 Discover diffractometer was used to estimate the evolution of Bi composition and layer thickness on the sample surfaces. Because different fluxes have different spatial distribution and the substrate temperature slightly changes at the wafer border, surface morphology and bismuth concentration are spatially inhomogeneous. The droplet-free section of the wafer was observed between −20 mm and +4 mm, and the droplets covered the rest of the wafer as shown in Figure 1. The thickness of the sample decreased along its length, because of the non-uniform distribution of the Ga flux on the immobile surface sample (i.e., left axis in Fig. 1). Bi content was measured to be maintained constant in the droplet area, whereas it increased on the left part of Figure 1.

A PL study performed on the piece of a sample corresponding to the position values of 0–5 mm has already been published.11 Here, the sample that was studied in this paper corresponded to the position values of 5–10 mm, the droplet-rich zone. It was expected that the presence of droplets does not significantly affect the optical properties of a GaAsBi layer. As a matter of fact, in this condition where droplets are formed, the rest of the layer is kept grown under minimal V/III flux ratio corresponding to the one for preserving III–V stoichiometry. This is the optimal growth condition for GaAsBi, as it has already been observed.15 PL optical emission should be close to that of the adjacent piece of the sample in part without droplets already reported by Mazzucato et al.11 In this paper,

our intention was not to explain droplet-formation, but to determine the nature of the defect and study the effect of droplet-formation on PL characteristic and effect of thermal annealing on droplet structure.

The droplet-rich sample that was studied here was split along its length into four pieces. Three of these pieces were submitted to rapid thermal annealing in AnnealSys AS-One equipment under a nitrogen flux. For annealing, the sample surface was protected with a GaAs piece to minimize As desorption at high temperature. A different temperature was applied to each piece as 750 C, 800 C and 850 C for 30 seconds. These high temperatures were employed to check how the droplet-rich GaAsBi layer reacted when annealed at such temperatures.

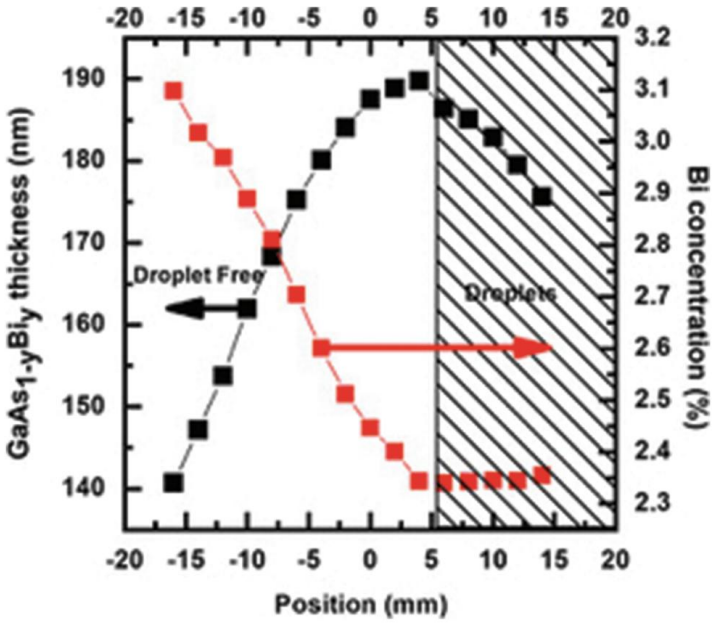

Figure 1. A map of the Bi content and layer thickness of the GaAsBi layer that was grown. Origin of the x-axis is the center of the wafer. The sample studied in this paper was taken from the hatched area of the wafer, which contained droplets.

In order to gain insight into the effects of annealing temperature, the surface morphologies of as-grown and annealed GaAsBi samples were monitored and analyzed by AFM (Park System, XE-100). The AFM measurements were obtained in the non-contact mode by using a silicon cantilever with the code NSC-15.

The etching process for the droplets was performed to check the effects of their presence on the optical properties of the layer and identify the nature of the droplets. Selective chemical etching procedure was separately made by dipping and stirring the samples in 1:4 dilute solutions (acid solution:de-ionized water) containing HCl (37%, Sigma Aldrich) for etching Bi and H2SO4 (38–40%, Sigma Aldrich) for etching Ga. After the chemical process, EFM measurements were carried out in an attempt to detect the presence of phase separation in the droplets. In order to take EFM images, a cantilever coated with Au/Cr (cantilever code: NSC-14) was used, and the backs of all samples were coated with 50-nm-thick Au. A 10 V voltage was applied between the cantilever and the sample during the EFM measurements.

In order to observe the effects of the chemical process on the optical properties of these samples, PL measurements were performed at room temperature. An Ar ion laser was used as an

excitation source, and the intensity of the laser was kept at 19.74 mWcm−2. The PL spectrum was dispersed by a 0.5 m focal length monochromator, detected by a photomultiplier tube and recorded by a lockin amplifier.

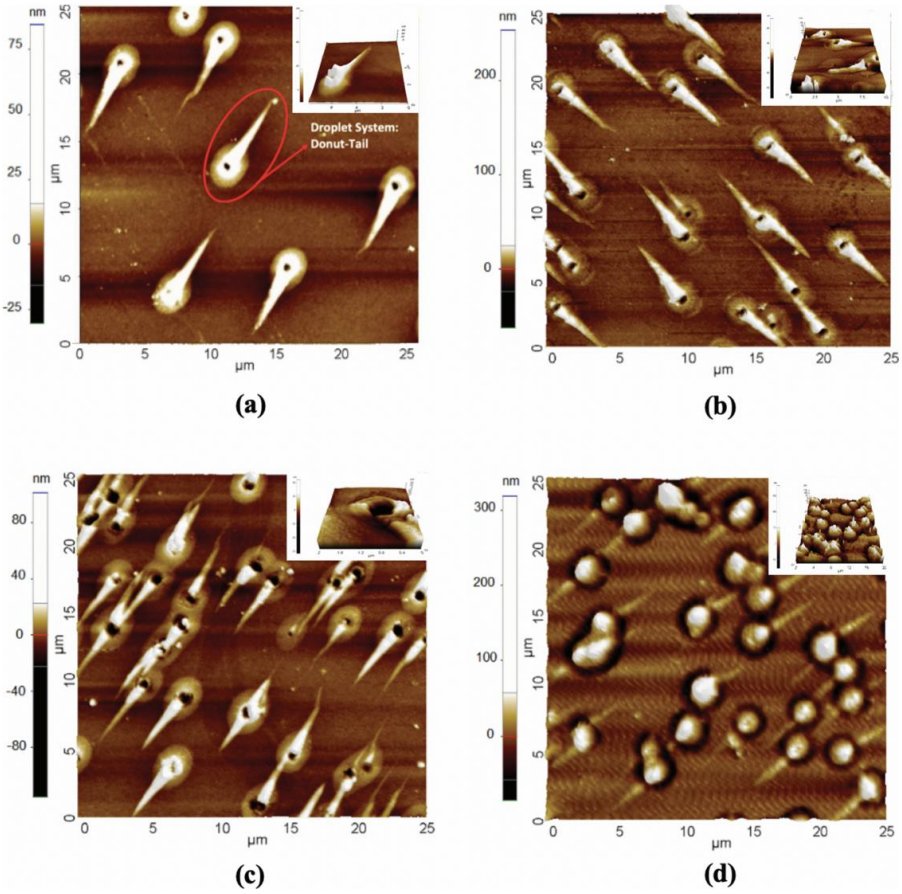

Figure 2. AFM images of the samples: (a) As-grown, (b) 750 C, (c) 800 C and (d) 850 C. (Imaging scale; 25 m×25 m). The inset at each 2D AFM image represents the 3D AFM. Image of the samples.

Sample	Total area (μm^2)	Total volume (μm^3)	Average diameter of disc (μm)	Average length of the tails (μm)	Average height of the droplets (μm)
As-grown	71	1.51	0.482	5.470	0.22
Annealed@750 °C	122	2.09	0.505	4.551	0.31
Annealed@800 °C	151	2.26	0.851	3.895	0.49
Annealed@850 °C	247	3.60	1.011	3.582	0.56

Table I. Annealing temperature dependence of some physical parameters for the droplet system microstructure on the surfaces of all samples— (Imaging scale; 25 m×25 m).

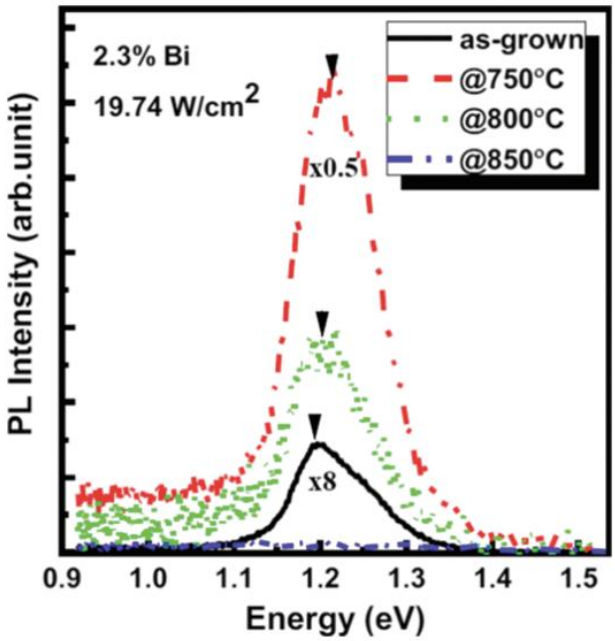

Figure 3. (a) PL intensity of the as-grown and annealed samples with a Bi content of 2.3% at 300 K under 19.74 mW/cm2 of excitation. Results on the scales of the as-grown sample and the sample annealed at 750 C are adapted for clarity.

3. RESULTS AND DISCUSSION

Figure 2 shows the AFM images of the surfaces of the as-grown and annealed samples. An observed droplet system was composed of a donut shape and with a tail. It was observed that the donut-like morphology changed, and the average tail was shortened by increasing the annealing temperature in some parts of the surface.

Analyzing the AFM results, we determined the area, volume and height of the droplet system for the as-grown and annealed samples as given in Table I. According to the values presented in Table I, the area and volume of the droplet systems increased with the annealing temperature, whereas the tail length decreased. The average height of the droplets measured from the surface increased as an influence of thermal annealing. The density of the droplets increased by increasing the annealing temperature except for the sample annealed at 850 C. As for the sample annealed at 850 C, the droplets gathered together. It is well-known that Bi and Ga fluxes, the growth rate/temperature and the V/III ratios play an essential role in the formation and density of droplet systems. Once droplet systems appear on the surface, they cannot be removed even if post thermal annealing is applied.9

In order to characterize the effects of the thermal annealing process on the optical properties of the alloy, PL measurements were performed. The PL spectra of the annealed samples reflected the very well-known asymmetrical emission lineshape that is usually observed for highly mismatched alloys (HMAs). PL emission peak broadening should result from composition inhomogeneity in the sample due to the use of a non-optimized growth condition leading to alloy clustering or alloy fluctuations.16

The PL emission peak was observed to become broader but more intense when the annealing temperature was increased to 750 C as shown in Figure 3. The higher annealing temperature than the annealing temperature optimized for GaAsBi epilayers with this Bi content

(2.3%) could account for the change in the lineshape.6 The samples that were used in a previous study15 and the one studied here were from the same wafer. For the droplet-free piece of a sample, Mazzucato et al.11 reported that PL emission was slightly improved after the thermal annealing process at 750 C, but PL peak energy did not change. In our case, we observed a blueshift of ∼46 meV, corresponding to ∼20 meV per %Bi. This, therefore, showed that the effect of the thermal annealing process was different from the one observed by Mazzucato et al. on the droplet-free section of the wafer. The growth conditions resulted in the formation of a droplet system and caused GaAsBi with droplets to reveal different optical properties.

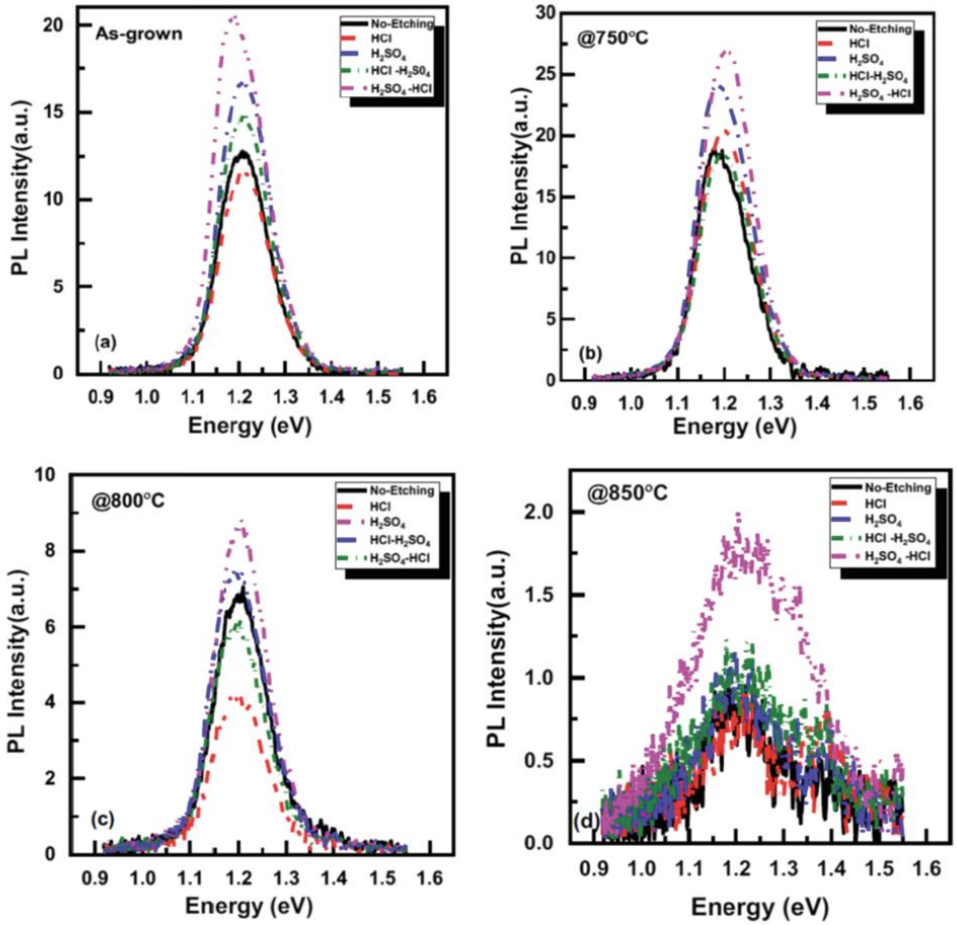

Figure 4. EFM phase images of GaBi0023As0077 annealed at 850 C. Imaging scale; 50 m × 50 m. (a) Not-etched, (b) HCl etched, (c) H2SO4 etched, (d) two-step etch with HCl+H2SO4, and (e) two-step etch with H2SO4 +HCl.

The observed blueshift may be explained regarding the change in the nearest neighboring configuration of a Ga– Bi cluster. Usman et al. proposed a theoretical model for Bi-related defect states in the bandgap.17 Using this model, Usman et al. calculated the effects of a pair of Bi atoms and different Ga–Bi cluster configurations, composed of three Bi atoms and one Ga atom called type I and two Bi atoms and one Ga atom called type II with different nearest-neighbor environments, on Bi-free GaAs bandgap edge. The calculated energies of a Bi-pair, the type I and the type II localized defects above the valence band edge were determined as 9.8 meV/Bi%, 36.8 meV/Bi% and 8.4 meV/Bi%, respectively.17 Therefore, the reason for the observed blueshift may be related to a change in the nearest neighbor configuration of Ga–Bi atoms or Bi-pairs inside the GaAsBi layer

In order to gain further insight into the droplet system's structure, we chemically etched all samples. It was reported that an HCl acid solution removes mostly Ga but also Bi from the surface,12 and an H2SO4 solution only attacks Bi.10 Therefore, we applied both HCl and H2SO4 to identify the

elemental composition of the droplets. Each sample was cleaved into two pieces. One piece was etched in an HCl solution, and the other part was etched in an H2SO4 solution. EFM images were taken after each etching step. Figure 4 shows the EFM phase signals that were obtained on the etched as-grown and annealed GaAs0077Bi0023 samples. It has been reported that if the growth is Ga-rich, the droplets may present a Ga–Bi structure.12 18 If the droplet-system consists of two different elements, the phase image of EFM reveals a phase separation. Moreover, the bright areas of an EFM image belong to the element with higher conductivity. The EFM images clearly showed that some areas of the droplets were brighter than the other sides. Since Bi has higher conductivity than Ga, the bright side of the EFM indicated the presence of Bi atoms in the relevant location of the droplet system.

According to the EFM images taken on the HCl-etched samples, some parts of the droplet-tail system could be etched from the surface. Since HCl can remove both Ga and Bi as reported in a previous study,12 it is not possible to conclude the elemental composition of the droplet as Ga or Bi. It is only known that it consists of Ga or Bi. It was observed that the center of the droplets was removed after the H2SO4 solution was used, which indicated that the center of the droplets was composed of Bi, but the tail side of the droplets was not affected by this process. Therefore, it may be concluded that the center of the droplet system consisted of Bi, but the tail section was Ga-rich. Since Bi is more metallic than Ga, the brighter areas observed in the EFM images corresponded to Bi-rich areas. To remove the whole droplet system from the surface, we also applied two-step chemical processes, by either H2SO4 + HCl or HCl+H2SO4. Both two-step processes were more efficient to remove the surface droplets and tails in comparison to the single step process with either H2SO4 or HCl as it may be seen from the EFM images and the data tabulated in Table II.

Table II shows the parameters of the droplet systems after different etching processes were applied. The average droplet heights were measured for all samples following each chemical process. It is clear that the average height of the droplets decreased for the annealed samples for all chemical etch steps. On the other hand, as for the as-grown sample, the increased average height measured between the top of the droplet and the surface that increased after the etching process with HCl indicates that HCl not only removed the droplets but also some part of the GaAsBi epilayer at around the center of the droplets. Because the average height of droplets was the smallest in comparison to that of the annealed samples, it could be expected that the chemical procedure etched more thickness, and the final form of the droplets could be considered as conic-shapes. The remaining total droplet area and volume were found to be the lowest for all samples in the case of this two-step etching. Therefore, it may be concluded that the most effective chemical process to remove the droplet system from the surface was the two-step process with H2SO4 +HCl. The EFM phase images are presented in Figure 4 for the sample annealed at 850 C before and after chemical etching was applied.

The effects of the chemical processes on the PL emission peaks of all samples are shown in Figure 5. PL measurements were carried out at room temperature under 19.74 Wcm−2 excitation power. The highest PL intensity was observed after etching by using the two-step chemical process with H2SO4 + HCl. On the other hand, the chemical processes involving HCl tended to decrease PL intensity. Two possible origins may be proposed to explain this PL signal improvement. Because surface droplet systems may behave as scatters, their removal is expected to increase the PL intensity signal in comparison to ones obtained on as-grown samples. The net surface of the sample pumped by the excitation laser increased as the droplet systems were etched. Therefore, the PL signal increased further. However, this result could also originate from the fact that the growth surface along GaAsBi growth is Bi-rich, with a floating Bi adlayer.19 This Bi excess could have been

suppressed using an in situ post-growth annealing process, but such a procedure was not applied to the investigated samples. The PL peak energy following the chemical processes did not change significantly. The two-step etch process with H2SO4 + HCl for the asgrown sample and the annealed samples at 750 C caused a slight shift, but evaluation of the origin of this shift was not easy because a high-resolution cross-section compositional analysis had to be carried out. However, because PL was quite broad, the degree of the shift could be ignored.

Sample	Etching process	Total area (μm^2)	Total volume (μm^2 deg)	Average height (μm) Before Chemical treatment	Average height (μm) After Chemical treatment
As-grown	HCl	33.6	460	0.22	0.21
	H_2SO_4	18.6	380		0.27
	HCl–H_2SO_4	12.0	277		0.32
	H_2SO_4-HCl	11.5	197		0.49
Annealed @750 °C	HCl	44.0	562	0.31	0.17
	H_2SO_4	33.8	432		0.23
	HCl–H_2SO_4	32.4	287		0.28
	H_2SO_4-HCl	27.4	242		0.32
Annealed @800 °C	HCl	53.0	684	0.49	0.16
	H_2SO_4	48.2	640		0.22
	HCl–H_2SO_4	45.3	623		0.25
	H_2SO_4-HCl	42.0	401		0.29
Annealed @850 °C	HCl	72.0	789	0.56	0.11
	H_2SO_4	69.0	765		0.35
	HCl–H_2SO_4	65.0	728		0.43
	H_2SO_4-HCl	58.0	700		0.51

Table II. Selective etching dependence of some physical parameters of the droplet system with droplet and tail measured for all samples from the EFM images; the line marked with blue shows the best results in this process (Imaging scale; 50 m×50 m).

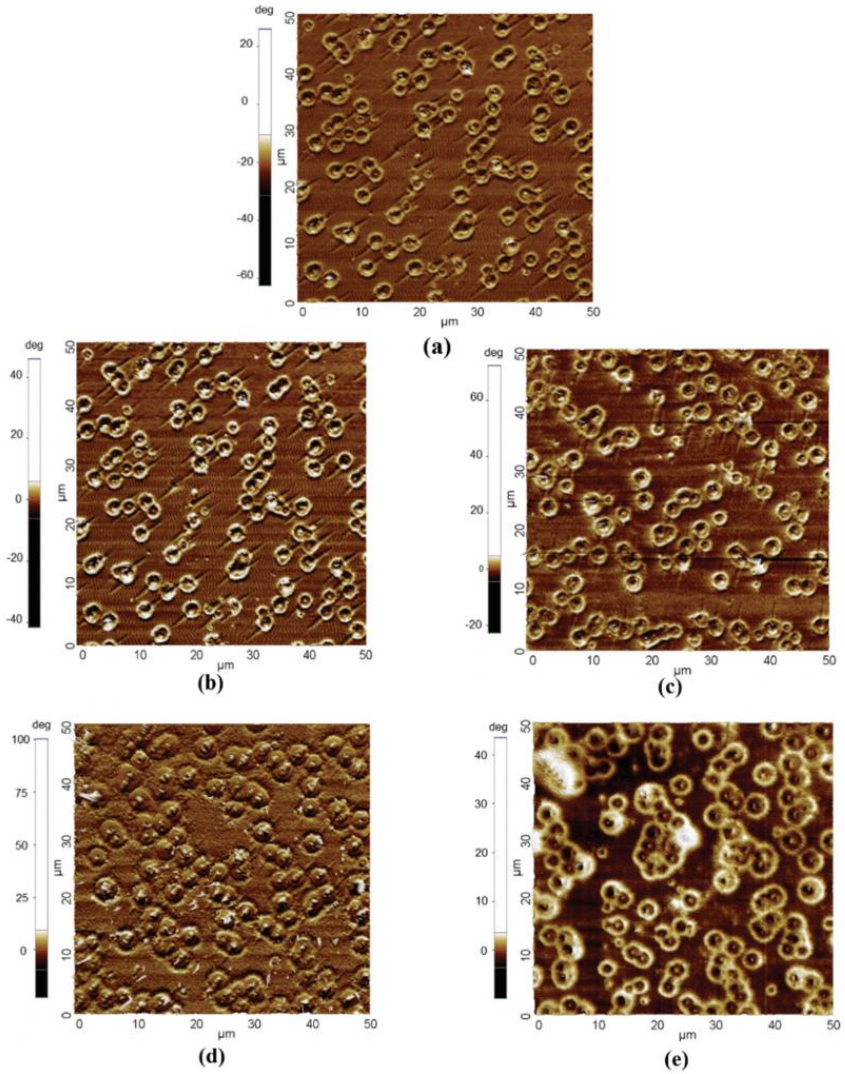

Figure 5. The effect of the selective etching process on the optical properties of the as-grown (a), annealed (750 C) (b), annealed (800 C) (c) and annealed (850 C) (d) GaBi0023As0077 epilayers.

4. CONCLUSION

We studied the optical and structural properties of GaAs0077Bi0023 samples with droplet systems using the AFM, EFM and PL techniques to investigate the effects of thermal annealing and selective etching processes on GaAsBi epilayers. The AFM results revealed that the droplet systems on the surfaces tended to accumulate towards the center, and the sizes of the droplet systems increased by increasing the annealing temperature. The EFM phase images showed the presence of phase separation in the droplet systems as Ga and Bi. The room temperature PL spectrum of the GaAsBi layer that was annealed at 750 C exhibited a higher-intensity emission and a negligible blueshift in comparison to the spectrum of the as-grown-sample.

A detailed analysis of the chemical etching procedure revealed that the most effective chemical process to remove droplet systems and improve the optical signal was the two-step H2SO4 +HCl etching process.

Acknowledgments:

This study is supported by Istanbul University Scientific Research Projects Unit (Project No. FYL-2016-20699, Project No: FYD-2016-20128, and Project No: ONAP-52321).

References and Notes

1. G. Vardar, S. W. Paleg, M. V. Warren, M. Kang, S. Jeon, and R. S. Goldman, Appl. Phys. Lett. 102, 042106 (2013).

2. K. Forghani, Y. Guan, A. W. Wood, A. Anand, S. E. Babcock, L. J. Mawst, and T. F. Kuech, J. Cryst. Growth 395, 38 (2014).

3. B. Fluegel, S. Francoeur, A. Mascarenhas, S. Tixier, E. C. Young, and T. Tiedje, Phys. Rev. Lett. 97, 067205 (2006).

4. S. Francoeur, M. J. Seong, A. Mascarenhas, S. Tixier, M. Adamcyk, and T. Tiedje, Appl. Phys. Lett. 82, 3874 (2003).

5. S. Tixier, M. Adamcyk, E. C. Young, J. H. Schmid, and T. Tiedje, J. Cryst. Growth 251, 449 (2003).

6. F. Gan, O. Kunishige, and Y. Masahiro, Jpn. J. Appl. Phys. 46, L764 (2007).

7. F. Sarcan, Ö. Dönmez, K. Kara, A. Erol, E. Akalın, M. Ç. Arıkan, H. Makhloufi, A. Arnoult, and C. Fontaine, Nanoscale Res. Lett. 9, 119 (2014).

8. A. Erol, E. Akalin, K. Kara, M. Aslan, V. Bahrami-Yekta, R. B. Lewis, and T. Tiedje, J. Alloys Compd. 722, 339 (2017).

9. I. Moussa, H. Fitouri, Z. Chine, A. Rebey, and B. E. Jani, Semicond. Sci. Technol. 23, 125034 (2008).

10. M. M. S. Nejad, Optical and Electronic Properties of GaAsBi Alloys for Device Applications, Canada, Ph.D. Thesis, University of British Columbia (2015).

11. S. Mazzucato, P. Boonpeng, H. Carrère, D. Lagarde, A. Arnoult, G. Lacoste, T. Zhang, A. Balocchi, T. Amand, X. Marie, and C. Fontaine, Semicond. Sci. Technol. 28, 022001 (2013).

12. O. M. Lemine, A. Alkaoud, H. Galeti, V. Orsi Gordo, Y. Gobato, H. Bouzid, A. Hajry, and M. Henini, Superlattice Microst. 65, 48 (2014).

13. H. Makhloufi, P. Boonpeng, S. Mazzucato, J. Nicolai, A. Arnoult, T. Hungria, G. Lacoste, C. Gatel, A. Ponchet, H. Carrère, X. Marie, and C. Fontaine, Nanoscale Res. Lett. 9, 123 (2014).

14. O. Donmez, K. Kara, A. Erol, E. Akalin, H. Makhloufi, A. Arnoult, and C. Fontaine, J. Alloys Compd. 686, 976 (2016).

15. R. B. Lewis, M. Masnadi-Shirazi, and T. Tiedje, Appl. Phys. Lett. 101, 082112 (2012).

16. S. Imhof, A. Thränhardt, A. Chernikov, M. Koch, N. S. Köster, K. Kolata, S. Chatterjee, S. W. Koch, X. Lu, S. R. Johnson, D. A. Beaton, T. Tiedje, and O. Rubel, Appl. Phys. Lett. 96, 131115 (2010).

17. M. Usman, C. A. Broderick, A. Lindsay, and E. P. O'Reilly, Phys. Rev. B 84, 245202 (2011).

18. B.-Y. Vahid, T. Thomas, and M. S. Mostafa, Semicond. Sci. Technol. 30, 094007 (2015).

19. X. Lu, D. A. Beaton, R. B. Lewis, T. Tiedje, and M. B. Whitwick, Appl. Phys. Lett. 92, 192110 (2008).